TRANSACTIONS
OF TIANJIN UNIVERSITY

2016, 22: 302-307
DOI 10.1007/s12209-016-2682-2

Effects of Strain Ratio on Fatigue Behavior of G20Mn5QT Cast Steel*

Han Qinghua(韩庆华)[1,2], Guo Qi(郭　琪)[1], Yin Yue(尹　越)[1,2], Xing Ying(邢　颖)[1]

(1. School of Civil Engineering, Tianjin University, Tianjin 300072, China;
2. Key Laboratory of Coast Civil Structure and Safety of Ministry of Education, Tianjin University, Tianjin 300072, China)

Abstract: Due to traffic and wave actions, cast steel joints are subjected to variable-amplitude fatigue loading, which may cause fatigue problems. The ratio of the minimum strain to the maximum strain (strain ratio) can be employed to analyze the influence of variable-amplitude fatigue both in the elastic and plastic ranges. To evaluate the effect of the strain ratio on G20Mn5QT cast steel, the fatigue tests of smooth specimens were carried out at the strain ratio of 0.1. The cyclic deformation and the relationships between the strain amplitude, the stress amplitude, the Smith, Watson and Topper (SWT) parameter and fatigue life were studied and compared with those at the strain ratio of −1. Compared with other methods, Basquin formula and Solonberg formula provide reliable and appropriate ranges of *S-N* curve and fatigue limit at different strain ratios respectively. The SWT parameter can be used to predict the fatigue life at other strain ratios accurately.

Keywords: fatigue test; G20Mn5QT cast steel; strain ratio; fatigue life

Cast steel joints have many advantages compared with unstiffened tubular joints. The welding area can be removed from the area which is less stressed and can be assembled easily. Therefore, the residual stress is prevented. In addition, cast steel joints have a flowing form without any sharp edge, so stress concentration and notch effects can be diminished efficiently. Joint geometry and wall thickness may be perfectly fit for the internal forces, thus the nominal stress can be reduced[1]. For the above reasons, cast steel joints have already been widely used in offshore platform structures (Fig. 1(a)), and now are increasingly applied in bridges (highway bridges and railway bridges) (Fig. 1(b)) and tall building structures (Fig. 1(c))[2]. In these applications, the wave loads, moving vehicle loads and wind vibration may cause serious fatigue problem.

(a) Platform structure　(b) Nesenbachtal Viaduct　(c) Hangzhou Bay Sightseeing Tower

Fig. 1　Cast steel joints

Accepted date: 2016-03-01.
* Supported by the National Natural Science Foundation of China (No. 51178307 and No. 51525803).
Han Qinghua, born in 1971, male, Dr, Prof.
Correspondence to Yin Yue, E-mail: yinyue@tju.edu.cn.

Fatigue failure usually occurs in the fillets of joints or butt-welded connection[3]. DNV[4] provided a reference for the fatigue analysis on offshore steel structures, including the *S-N* curves of offshore steel and welded structures, hot spot stress method and fracture mechanics method. IIW[5] offered the *S-N* curves of welded structures made of steel and aluminum. Low cycle fatigue behavior of magnesium alloys with different strain ratios was also analyzed[6,7]. However, the cast steel joints in civil engineering vary a lot from those in offshore structures in environmental conditions, geometric profiles, welding details and casting process, which leads to a different fatigue behavior. In China, Ref. [8] only recommended the material properties of cast steel but barely fatigue properties; Ref. [9] analyzed the fatigue behavior of G20Mn5QT cast steel in civil engineering under fully reversed total strain amplitude control conditions. Structures usually bear a changeable fatigue load, but little attention has been paid to the fatigue behavior of structural cast steel at different strain ratios, R_ε, which equals the ratio of the minimum strain to the maximum strain.

In this study, fatigue tests were carried out on the smooth specimens of G20Mn5QT cast steel at $R_\varepsilon = 0.1$. The evolutions of the stress-strain curve and cyclic response were analyzed. The strain-life curves were compared with those at $R_\varepsilon = -1$. The methods which consider the influence of the mean stress were compared, and the Smith, Watson and Topper (SWT) parameter can be used to predict appropriate fatigue life.

1 Experimental details

Test specimens were made of G20Mn5QT cast steel tubes of Φ 219 mm × 32 mm, which were specially manufactured for the test with general manufacture process (shown in Fig. 2). Material tests of chemical composition and mechanical properties were conducted, and the results are shown in Tab. 1 and Tab. 2. All the test results met the requirements for G20Mn5QT cast steel in Ref. [8] and Ref. [10].

Tab. 1 Chemical composition (mass fraction) **of G20Mn5QT cast steel** %

Source	C	Mn	Si	S	P	Ni
Tests	0.17	1.16	0.34	0.018	0.02	0.039
Ref. [10]	0.17—0.23	1.00—1.60	⩽ 0.60	⩽ 0.02	⩽ 0.02	⩽ 0.80

Tab. 2 Mechanical properties of G20Mn5QT cast steel

Source	Yield strength/MPa	Tensile strength/MPa	Elongation/%	Yield strain	Tensile strain	Reduction of area/%
Tests	351.87	521.44	28.93	0.001 9	0.17	63.59
Ref. [10]	⩽300	500—650	⩾ 22	—	—	—

Compared with the stress-based method, the strain-based method considers the plastic deformation that may occur in the localized regions where fatigue cracks initiate. The strain-based method can address both low and high cycle fatigue problems and account directly for the difference in concentrations among different fatigue details[11]. The stress of materials in structures is commonly designed within the elastic range, or near the yield value in some special conditions. Therefore, the fatigue tests were conducted with Instron ElectroPuls E10000 all-electric test instrument with a strain range ($\Delta\varepsilon$) of 0.10%—0.20%. A 10 mm-long extensometer was clipped on the gauge-length section of the specimen as shown in Fig. 3. A symmetrical sinusoidal waveform strain load was applied on the specimens during the test at $R_\varepsilon = 0.1$, the loading frequency was 10 Hz, and the testing temperature was room temperature (23 ℃).

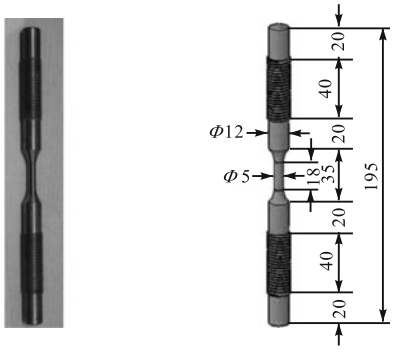

(a) Photograph (b) Geometric dimensions in mm

Fig. 2 Fatigue test specimen

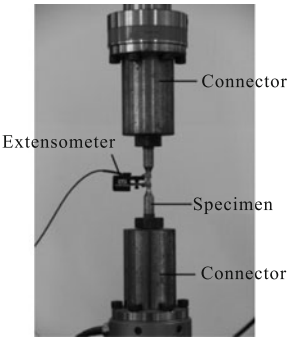

Fig. 3 Fatigue test setup

2 Results and discussion

2.1 Cyclic deformation

The evolutions of the stress-strain curves at $R_\varepsilon = 0.1$ and – 1 are shown in Fig. 4, while the data with N_i larger than $0.1N_f$ are not exhibited because the stress-strain curves keep stable after that, where N_i and N_f are the number of current cycles and fatigue cycles respectively. For the curves at $R_\varepsilon = -1$, it can be seen from Fig. 4 that nearly all the stress-strain curves are symmetric to the origin. As the number of loading cycles increases, the curves mainly keep stable. For the curves at $R_\varepsilon = 0.1$, although the minimum strain is positive, there are still negative stress values. With the decrease of strain amplitude, the curves reach the stable condition more quickly.

The relationship between the stress amplitude σ_a and fatigue life fraction N_i/N_f at different strain amplitudes (ε_a) is shown in Fig. 5. For the specimens at $R_\varepsilon = -1$, the curves nearly maintain a stable response during all the fatigue life until 0.8 N_f—1.0 N_f. However, for the specimens at $R_\varepsilon = 0.1$, the curves exhibit only a little hardening during 0—$0.1N_f$, and then keep stable until fracture. As shown in Fig. 6, with the same strain amplitudes (ε_a = 0.1%), the specimens at $R_\varepsilon = 0.1$ show bigger stress amplitudes and mean stresses than those at $R_\varepsilon = -1$. With the increasing number of loading cycles, all kinds of stresses at $R_\varepsilon = -1$ remain constant during the whole stage of life, while both the maximum and minimum stresses decline slightly during 0—$0.1N_f$ and lead to a small decrease of mean stress at $R_\varepsilon = 0.1$. In general, there is no obvious softening or hardening behavior under the loads that structures commonly bear.

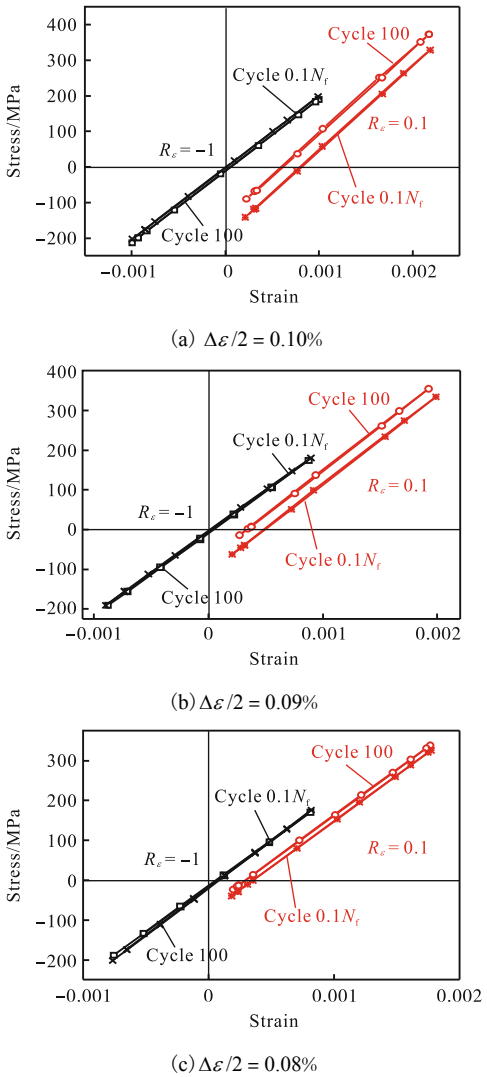

Fig. 4 Evolution of stress-strain curves at $R_\varepsilon = 0.1$ and –1

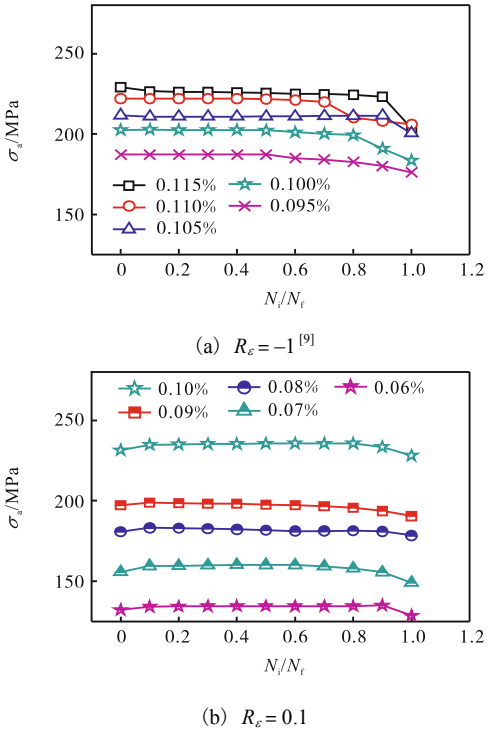

Fig. 5 Stress amplitude vs fatigue life fraction at different strain amplitudes

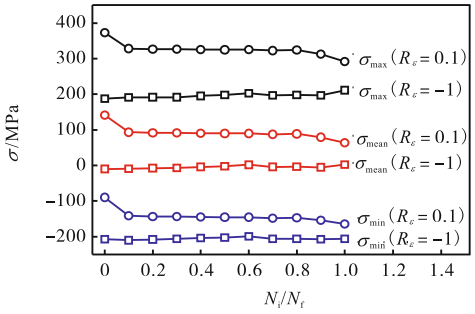

Fig. 6 Variations of the maximum stress, minimum stress and mean stress with increasing number of loading cycles for ε_a = 0.1%

2.2 ε_a-N_f curves

The fatigue life N_f, strain amplitude ε_a, controlled maximum strain ε_{max}, minimum strain ε_{min} and the corresponding stress amplitude σ_a of 11 specimens at $R_\varepsilon = 0.1$ are listed in Tab. 3. The relationship between ε_a and N_f is shown and regressed linearly in Fig. 7, and compared with that at $R_\varepsilon = -1$[9]. The arrows in the figure indicate the run-out data, with their fatigue lives longer than 1×10^7. The fatigue limit at $R_\varepsilon = -1$ and 0.1 can be determined to be 0.092 5% and 0.05% respectively based on the test data. With the same strain amplitude, the specimens at $R_\varepsilon = 0.1$ possess a shorter fatigue life than those at $R_\varepsilon = -1$ because of the relatively bigger ε_{max}. All the stresses of the specimens are within the elastic range or near the yield value. The parameters of Coffin-Manson equation cannot be regressed precisely, therefore, the influence of the strain ratio cannot be expressed exactly by the equation.

Tab. 3 Fatigue data of G20Mn5QT cast steel at $R_\varepsilon = 0.1$

ε_a/%	ε_{max}/%	ε_{min}/%	σ_{max}/MPa	σ_a/MPa	N_f
0.10	0.220	0.022	325.27	217.72	26 530
0.10	0.220	0.022	309.42	235.53	62 805
0.09	0.200	0.020	320.86	197.54	35 348
0.09	0.200	0.020	324.96	211.76	90 940
0.08	0.180	0.020	315.60	181.56	493 007
0.08	0.180	0.020	200.78	157.18	1 539 642
0.07	0.156	0.016	246.79	160.04	745 312
0.07	0.156	0.016	284.76	159.08	1 800 000
0.06	0.133	0.013	253.23	140.31	2 543 825
0.06	0.133	0.013	258.12	134.50	750 000
0.05	0.110	0.010	249.92	113.09	1×10^7

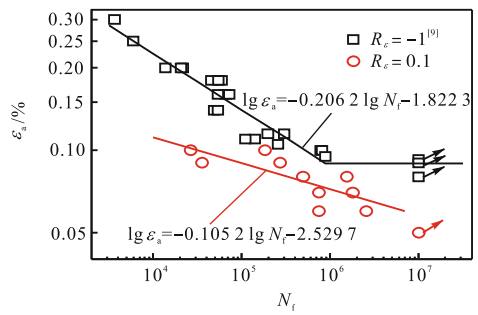

Fig. 7 Strain amplitude vs fatigue life for G20Mn5QT cast steel at $R_\varepsilon = 0.1$ and –1

2.3 *S-N* curves

As the stress amplitudes almost keep stable within the whole period of the fatigue life, ε_a-N_f curves can be changed into *S-N* curves. The fatigue life of the smooth specimen and the stabilized stress amplitude obtained at half of the fatigue life are presented in Fig. 8 for G20Mn5QT cast steel at $R_\varepsilon = -1$[9] and 0.1[11]. The relationship between the stress amplitude and fatigue life is regressed by the solid lines, and expressed as Eq. (1) and Eq. (2).

For $R_\varepsilon = -1$,

$$\lg\sigma_a = -0.090\ 8 \lg N_f + 2.841\ 9 \quad (1)$$

For $R_\varepsilon = 0.1$,

$$\lg\sigma_a = -0.107\ 14 \lg N_f + 2.842\ 4 \quad (2)$$

According to Ref. [4], the stress range or stress amplitude may be reduced if part of the stress cycles is in compression. The reduction factor f_m can be derived from the following equation:

$$f_m = \frac{\sigma_t + 0.6\sigma_c}{\sigma_t + \sigma_c} \quad (3)$$

where σ_t and σ_c are the maximum tension stress and maximum compression stress, respectively; f_m is 0.8 for the specimens at $R_\varepsilon = -1$, while ranges from 0.876 to 0.979 for the specimens at $R_\varepsilon = 0.1$ according to the tests. Based on the reduction factors, the range of *S-N* curve for $R_\varepsilon = 0.1$ can be calculated and plotted by the dotted lines in Fig. 8.

The mean stress is nearly zero for the specimens at

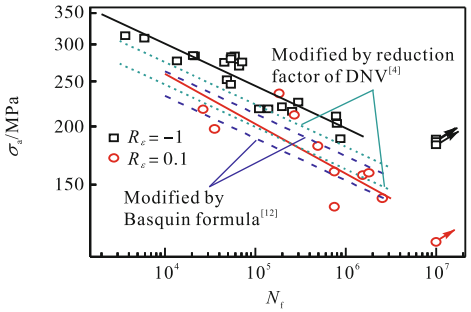

Fig. 8 Stress amplitude vs fatigue life for G20Mn5QT cast steel at $R_\varepsilon = 0.1$ and –1

$R_\varepsilon = -1$, while the value ranges from 64 MPa to 158 MPa for the specimens at $R_\varepsilon = 0.1$. The range of *S-N* curve at $R_\varepsilon = 0.1$ is calculated by the modified Basquin formula (Eq. (4)) [12], which is plotted by the dashed lines in Fig. 8.

$$\sigma_a = (\sigma'_f - \sigma_m)(2N_f)^b \tag{4}$$

where σ_m is the mean stress; σ'_f and b are the fatigue strength coefficient and fatigue strength exponent respectively.

It can be seen from Fig. 8 that the lines regressed by the experimental data are within the dashed lines, while the dotted lines cannot predict the range accurately. It is proved that the Basquin formula provides a more reliable reference for the prediction of the influence of the mean stress on the fatigue life than the DNV reduction factor.

The fatigue limits of the specimens at $R_\varepsilon = -1$ and 0.1 are respectively 188 MPa and 113 MPa. The range of fatigue limit of the specimens at $R_\varepsilon = 0.1$ was analyzed with three methods according to the range of the mean stress, as shown in Tab. 4, where $S_{a(R)}$ and σ_{-1} are the fatigue limits of stress ratio R and $R = -1$, respectively; S_m, σ_b and $\sigma_{0.2}$ are the mean stress, tensile strength and proof stress respectively. Because most of the specimens are still within the elastic range under the cyclic loads, the Solonberg formula which uses proportional limit may provide a more appropriate and conservative range, compared with the other two methods.

Tab. 4 Comparison among three methods of calculating fatigue limit

Method	Formula	Range of fatigue limit/MPa	
		Max	Min
Goodman	$S_{a(R)}/\sigma_{-1} = 1 - S_m/\sigma_b$	130	164
Geber	$S_{a(R)}/\sigma_{-1} = 1 - (S_m/\sigma_b)^2$	170	184
Solonberg	$S_{a(R)}/\sigma_{-1} = 1 - S_m/\sigma_{0.2}$	103	153

2.4 SWT-N_f curves

Although Basquin and Solonberg formula can offer the ranges of *S-N* curve and fatigue limit, the prediction is still not accurate. Therefore, SWT parameter is introduced, as shown in Eq. (5). Fig. 9 shows the SWT parameter versus the corresponding fatigue life for all the specimens tested at two different strain ratios.

$$\text{SWT} = \varepsilon_a \langle \sigma_{max} \rangle \tag{5}$$

where ε_a is the strain amplitude; the symbol $\langle\ \rangle$ is defined as $\langle x \rangle = 0.5(x + |x|)$, which is to make sure that the stress is non-negative. It should be noticed that the SWT parameter has a great advantage of having no material constant needed[6].

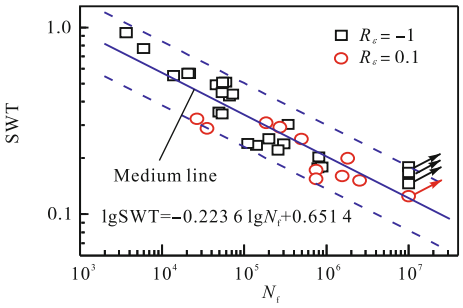

Fig. 9 SWT parameter vs fatigue life for G20Mn5QT cast steel at $R_\varepsilon = 0.1$ and -1

The fatigue data are presented in double log scales. The solid straight line is an approximate medium line of the SWT-N_f curve for all the test specimens, and the two dashed lines are the two boundaries. Clearly, the SWT parameter fits well with the uniaxial tension-compression experiments at different R_ε. The SWT parameter and fatigue life have a logarithmic relationship and were lineally regressed by Eq. (6). Therefore, with Eq. (6), the SWT parameter can predict the fatigue life appropriately.

$$\lg \text{SWT} = -0.223\,6 \lg N_f + 0.651\,4 \tag{6}$$

3 Conclusions

The fatigue tests of smooth specimens made of G20Mn5QT cast steel were carried out under total stain control at $R_\varepsilon = 0.1$ in ambient air and at room temperature. The fatigue properties including cyclic deformation, strain amplitude vs fatigue life, stress amplitude vs fatigue life and SWT vs fatigue life were studied, and compared with those at $R_\varepsilon = -1$. The following conclusions can be drawn.

(1) With the controlled strain ranging from 0.10% to 0.20%, the G20Mn5QT cast steel exhibits cyclic stability during the whole fatigue period at $R_\varepsilon = 0.1$ and -1.

(2) The ε_a-*N* curves and *S-N* curves were obtained from the tests. Compared with the method of reduction factor according to DNV, Basquin formula provides a more reliable reference considering the influence of mean stress.

(3) In comparison with the formulas of Goodman and Geber, Solonberg formula shows a more appropriate range of fatigue limits.

(4) The fatigue life calculated with the SWT pa-

rameter investigated in this study was proved to fit the fatigue test results well. The method provides a useful tool to predict appropriate fatigue life.

References

[1] Schober H. Cast steel joints for tubular structures[C]. In: *The 10th International Symposium on Tubular Structures*. Madrid, Spain, 2003: 143-152.

[2] Jin H, Li J, Mo J *et al*. Fatigue of girth butt weld for cast steel node connection in tower structure under wave loadings[J]. *Structural Design of Tall and Special Buildings*, 2014, 23(15): 1119-1140.

[3] Chen H, Zhang Q, Jin H. Experimental study on fatigue properties of cast-steel joints of Hangzhou Bay Sightseeing Tower[J]. *Journal of Building Structures*, 2009, 30(5): 149-154(in Chinese).

[4] Det Norske Veritas. Recommended Practice DNV-RP-C203 Fatigue Design of Offshore Steel Structures[S]. 2011.

[5] International Institute of Welding(IIW). IIW Document XIII-1965-03/ XV-1127-03 Recommendations for Fatigue Design of Welded Joints and Components[S]. Paris, France, 2003.

[6] Yu Q, Zhang J, Jiang Y *et al*. Effect of strain ratio on cyclic deformation and fatigue of extruded AZ61A magnesium alloy[J]. *International Journal of Fatigue*, 2012, 44: 225-233.

[7] Begum S, Chen D L, Xu S *et al*. Effect of strain ratio and strain rate on low cycle fatigue behavior of AZ31 wrought magnesium alloy[J]. *Materials Science and Engineering A*, 2009, 517(1/2): 334-343.

[8] Tongji University. CECS 235: 2008 Technical Specification for Application of Connections of Structural Steel Casting[S]. China Planning Press, Beijing, 2008(in Chinese).

[9] Han Q, Guo Q, Yin Y *et al*. Fatigue behaviour of G20Mn5QT cast steel and butt welds with Q345B steel[J]. *International Journal of Steel Structures*, 2016, 16(1): 139-149.

[10] European Committee for Standardization(CEN). DIN EN 10293 Steel Castings for General Engineering Uses[S]. Berlin, Germany, 2005.

[11] Chen H, Grondin G Y, Driver R G. Characterization of fatigue properties of ASTM A709 high performance steel[J]. *Journal of Constructional Steel Research*, 2007, 63(6): 838-848.

[12] Zheng X, Wang H, Yan J *et al*. *Fatigue Theory of Materials and Engineering Applications*[M]. Science Press, Beijing, China, 2013(in Chinese).

(Editor: Liu Wenge)